Materials Science Forum Vols. 715-716 (2012) pp 502-507
Online available since 2012/Apr/12 at www.scientific.net

doi:10.4028/www.scientific.net/MSF.715-716.502

Substructure Dynamics in crystalline materials: New insight from in-situ experiments, detailed EBSD analysis of experimental and natural samples and numerical modelling

Sandra Piazolo[1, a], Verity Borthwick[1,b], Albert Griera[2,3,c], Maurine Montagnat[4,d], Mark W. Jessell[2,e], Ricardo Lebensohn[5,f], Lynn Evans[6,g]

[1] Stockholm University, SWEDEN

[2]Paul-Sabatier, Toulouse, FRANCE

[3]Universitat Autònoma de Barcelona, SPAIN

[4]LGGE-UJF-CNRS, Grenoble, France

[5]Los Alamos National Laboratory, USA

[6]University of Melbourne, AUSTRALIA

[a]sandra.piazolo@geo.su.se, [b]verity.borthwick@geo.su.se, [c]albert.griera@uab.cat, [d]maurine@lgge.obs.ujf-grenoble.fr, [e]mark.jessell@lmtg.obs-mip.fr, [f]lebenso@lanl.gov, [g]laevans@unimelb.edu.au

Keywords: substructure, EBSD, in-situ experiments, numerical modelling, minerals, metals

Abstract. The understanding of the dynamics of substructures during deformation and annealing is fundamental in our ability to predict microstructural and physical properties such as rheological behaviour of crystalline materials. Here, we present an overview of new insights into substructure dynamics through a combination of in-situ heating experiments, detailed Electron Backscatter Diffraction (EBSD) analysis and numerical modelling.

Our main findings are summarised as follows:

A) In-situ annealing of substructure-rich, near isotropic minerals such as NaCl show distinct temperature dependent behaviour.

B) A numerical approach in which a lower energy state is achieved by local adjustment i.e. rotation of crystalline materials enables us to reproduce the experimentally observed, temperature dependent substructure dynamics observed in A).

C) Microstructures observed in a material with a highly anisotropic viscoplastic behaviour, i.e. ice, point to direct stress translations across grain boundaries, closely related grain boundary asperities and subgrain boundary tips, arrays of quasi-parallel subgrain boundaries frequently crossing whole grains; some of which are developed as kink-bands.

D) Development of a numerical simulation system which is able to predict deformation induced substructure development and recrystallization in crystalline material, including highly anisotropic material such as ice. Comparison between model and experiments enables the researcher to refine the interpretation of microstructures observed in C).

Through the combination of in-situ experiments and numerical modelling it is now possible to develop an in-depth understanding of subgrain scale processes as well as establish numerical models which reproduce the experimental observations. These can be utilised to predict microstructural development and rheological behaviour of a large variety of crystalline materials.

Introduction

In materials deformed by crystal plasticity a substructure of subgrain walls and dislocations develops. Such substructures are useful as indicators of active deformation and annealing mechanisms. Moreover, dislocation substructures have an important control on the mechanical

properties of materials. A thorough understanding of the nature of substructures is, therefore, needed to properly (a) describe and (b) predict the flow properties of materials deforming by dislocation processes and/or changing during annealing.

Over the past five decades, substantial insight has been gained into nano- to micro-scale processes in materials [1]. Here, we report some of the results of an initiative that aims to significantly improve our knowledge of dynamics of substructure formation and evolution in rocks and metals by breaking the traditional barriers that exist between the methodologies of classical and *in-situ* experiments, and numerical modelling. Time series obtained from *in-situ* experiments are crucial for the validation and extension of numerical simulations, as such experiments provide significantly more constraints for modelling than the post-mortem examinations available from traditional experimental approaches.

In this contribution, we present two integrated case studies investigating the nature of substructural development:

1) during annealing after viscoplastic deformation in the near isotropic material NaCl and
2) during deformation in the highly anisotropic material ice.

Through this work, we were able to develop numerical models with which it is possible to reproduce to a large extent the substructural development of the respective experiments. Furthermore, refinement of interpretations is possible by comparison of experimental and numerical results.

Methods

Electron Backscatter Diffraction (EBSD) analysis. Crystallographic data were collected using the SEM based EBSD technique [2]. Analyses were performed on uncoated samples at Stockholm University (Phillips XL-30 FEG-ESEM; Channel 5 analysis suite (Oxford instruments HKL Technology)) using a 12 or 20 kV accelerating voltage, working distance of about 20 mm under high vacuum mode. An average of 80 % EBSD patterns were automatically indexed, subsequent data processing followed the procedure described in [3]. For further details including preparation of ice samples the reader is referred [4,5,6].

Physical experiment I: In-situ heating of predeformed NaCl. The initial high purity NaCl single crystal (~7x10x15mm^3) was cleaved along {100} face before deformation. The geometry was chosen to activate one set of slip planes more easily during uniaxial deformation (453 ºC, final strain: 16.5%, strain rate: $6.9 \times 10^{-6} s^{-1)}$. For in-situ annealing experiments the pre-deformed single crystals were heated under high vacuum to temperatures of 280-470±15 ºC in a number of steps.

Physical experiment II: Uniaxial deformation of polycrystalline ice. We deformed polycrystalline columnar ice to avoid three dimensional effects. The ice was grown by directional solidification resulting in c-axes approximately perpendicular to the crystal growth and an average grain diameter of ~10 mm. Specimens (50x50x10mm^3) were deformed to a strain of 2-4% under uniaxial compression at -11ºC±1ºC, at a constant load of 0.5 MPa applied perpendicular to the column axes. To obtain orientations over the whole specimen, we performed analyses using the Automatic Ice Texture Analyser [7] constructing mosaics of 10 x 10mm^2 sections. Areas to be investigated with high resolution EBSD were cut out of the deformed crystalline aggregate.

Numerical modelling. We used the microdynamic modelling platform *Elle* [8, 9] for case study 2 and for case study 1 *Elle* in combination with a full-field crystal plastic code based on the Fast Fourier Transform method (FFT; [10]). In *Elle* several concurrent microstructural processes active at grain/subgrain scale can be simulated under dynamic (i.e. to high strain) and static conditions. The position of grains is defined by boundary nodes (bnodes) that delimit closed polygons. To specify variations within a polygon, e.g. orientation of crystallographic axes, a set of unconnected nodes (unodes) is introduced. To avoid boundary effects, all boundaries are periodic. During simulations bnodes are moved in small increments and the physical properties at the bnode and unode level are constantly adjusted according to given laws. For case study 1 recovery within an

individual grain is modelled in detail. Here, the basis for the rotation of individual unodes is the maximum energy reduction, where the energy is calculated using the theoretical considerations of diffusion-accommodated grain rotation provided by Moldovan et al. [11, 12]. Initial microstructures are directly taken from the relevant physical experiment. For case study 2 the numerical scheme involves crystal plastic deformation, nucleation, grain boundary migration and recovery as modelled in case study 1 (Fig. 1). The evolution of the local misorientation (deriving from the local and plastic spins of the crystallographic lattice associated with the unodes calculated with the FFT method) is used to calculate the corresponding geometrically-necessary dislocation density, which in turn is employed to predict the recrystallisation. Grain boundary curvature and stored strain energies are used as driving forces for grain boundary migration. Dislocation creep was simulated using a rate-sensitive approach (n=3) where deformation is mainly accommodated by basal slip with minor contribution by prismatic and pyramidal systems with a critical resolved shear stress contrast of M=20.

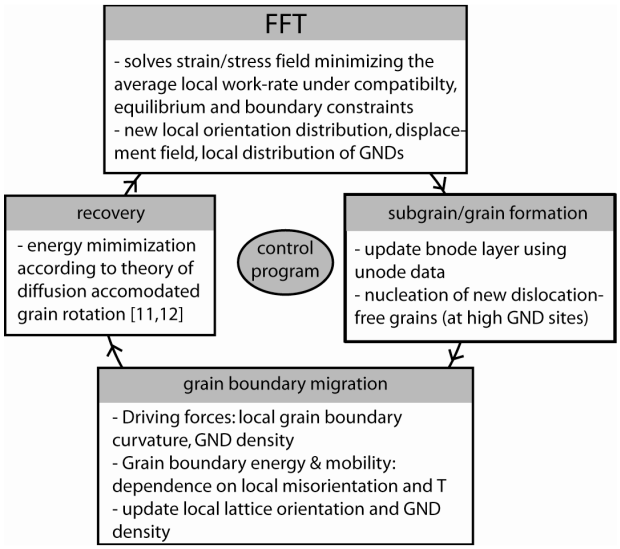

Figure 1: Numerical scheme for crystal plastic deformation combining FFT (full field crystal viscoplastic) and Elle code (case study 2). GND: geometrically necessary dislocations

Results and Discussion

Case Study 1: Substructure development during annealing in pre-deformed NaCl. In-depth analysis of in situ annealing experiments enabled us to (a) verify that some well-developed subgrain boundaries move during annealing (Fig. 2a-c) and (b) distinguish three temperature dependent regimes primarily based on boundary misorientation changes (Fig. 2f). During regime I (280-300 ºC) some low angle boundaries (LABs) increase in misorientation angle, while others decrease. During regime II (~300 ºC) all LABs undergo a decrease in misorientation angle (Fig. 2f). Regime III (>300 ºC) results in enhancement of the subgrain structure as remaining LABs increase. Throughout regimes I and II, new LABs develop, subdividing subgrains (Fig. 2d&e).

We suggest that three main processes are occurring during annealing (Fig. 2f),

1) Annihilation, as dislocations of opposite signs meet along the lattice planes. This process is most prominent during regime I and II.
2) In areas where dislocations of opposite sign are not available, dislocations of like sign begin to align into tilt walls, resulting in the subdivision of subgrains and formation of new LABs. By annealing regime III there are not enough free dislocations to initiate any new LAB formation; therefore such subdivision is only effective in regimes I and II.
3) Subgrain boundary movement; this process is active throughout all three regimes.

However, it is not immediately obvious why some boundaries should decrease and others increase in misorientation. In order to investigate the underlying physical law for this behaviour we have performed numerical simulations. Results from numerical simulations and experiments correspond very well. The observed behaviour with regard to increasing and decreasing subgrain boundaries as well as subdivision of subgrains are reproduced reliably with the simulation used (Fig. 3).

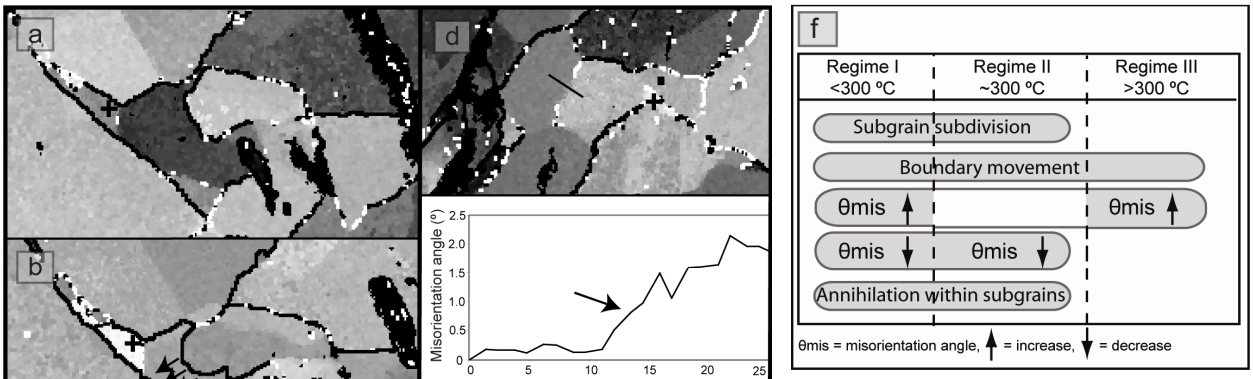

Figure 2: Substructure development in NaCl during annealing; a)-c) show subgrain boundary movement (black arrows); a) before heating, b) after heating ~2hr at 300 ºC, c) after heating ~6hr at 300-400 ºC; legend and scale bar are shown in (c). d) and e) Formation of new subgrain boundaries by subgrain sub-division, where two parts of the subgrain rotate away from one another to form areas of like orientation separated by a LAB; (d) before heating, (e) after heating 4hr at 280–455 ºC. Graphs beneath each image show misorientation transects (left-right) along the black line in map.

In (e) the transect shows subgrain boundary formation (black arrows);a-e) depict relative deviation in orientation with respect to a reference orientation (black cross); subgrain boundaries 1.5-2º, >2º are shown in white and in black, respectively. f) Schematic diagram showing which processes occur during each of the temperature dependent regimes.

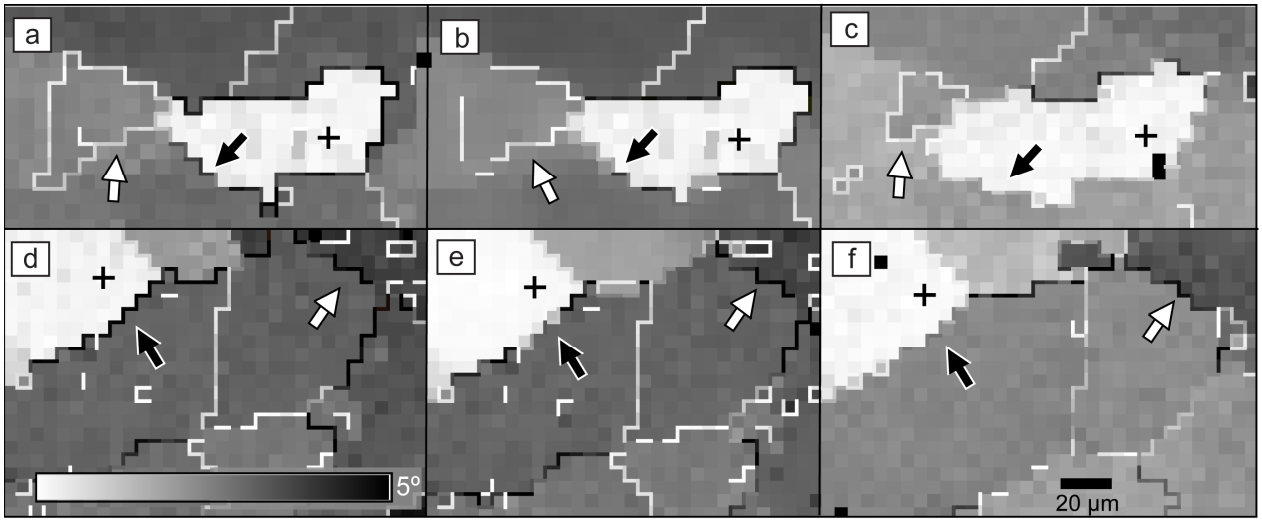

Figure 3: Comparison of numerical simulation with experimental results. a) and d) are before heating and simulation, b) and e) after running the simulation for 40 steps and c) and f) show experimental data after heating for ~5hr and 20min at 280-455 ºC. All images depict relative deviation in orientation with respect to a reference orientation (marked with a black cross in each). Angular deviation and a scale bar for all maps is shown under (d) and (f), respectively. Subgrain boundaries are coloured in greyscale with misorientations between 1º and 4º in a continuous colour gradient from white to black. a-c) Black arrows show a subgrain boundary which decreases in misorientation angle during heating; white arrows points to a subgrain boundary decreasing in misorientation resulting in a less well defined subgrain. d-f) follows another area where black arrows show a boundary which decreases in misorientation in both simulation and experiment. White arrows show a boundary which remained constant in misorientation and location.

Case Study 2: Substructure development in ice during viscoplastic deformation. Both from analysis of the complete deformed sample and from detailed EBSD analysis (Fig. 5) the following features are observed: (a) direct stress translations across grain boundaries (Fig. 4a), (b) subparallel

subgrains crossing whole grains which are sometimes developed as kink-bands (Fig. 5a) similar to those observed by [13] and (c) discontinuous subgrain boundaries at grain boundary asperities and triple points (Fig. 5b).

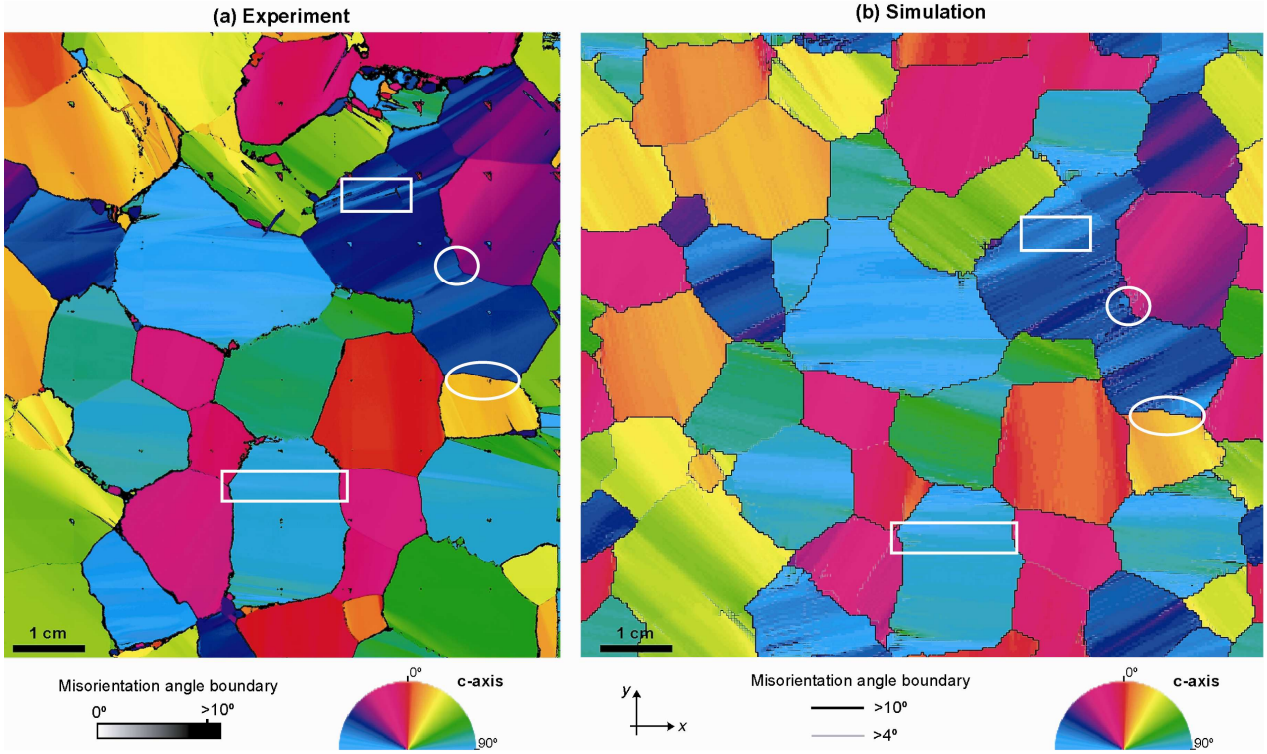

Figure 4 Comparison of a) physical experiment and b) simulation of ice deformation after a vertical strain of 4%. Note the first order correspondence of the results. White circles and boxes depict example areas for stress translation i.e. continuation of subgrain boundaries across a grain boundary and subparallel subgrains crossing whole grains, respectively. Colours indicate the orientation of c-axis; subgrain boundaries >4º, >10ºare shown in grey and black.

Numerical simulation result show a first order coherence with experiments (Fig. 4, 5, 6). Analysis of numerical experiments in which we can easily analyse the microstructural evolution by looking at different time steps show that the discontinuous subgrain boundaries do not *originate* at grain boundary asperities, in contrast asperities form due to grain boundary migration where subgrain boundaries were initiated due to differences in local dislocation density (Fig. 6). Numerical simulations predict slightly higher misorientation across subgrain boundaries than experimentally observed. This can be directly related to the difference in resolution of the numerical model and experimental data (~ 25 μm versus 1-5 μm).

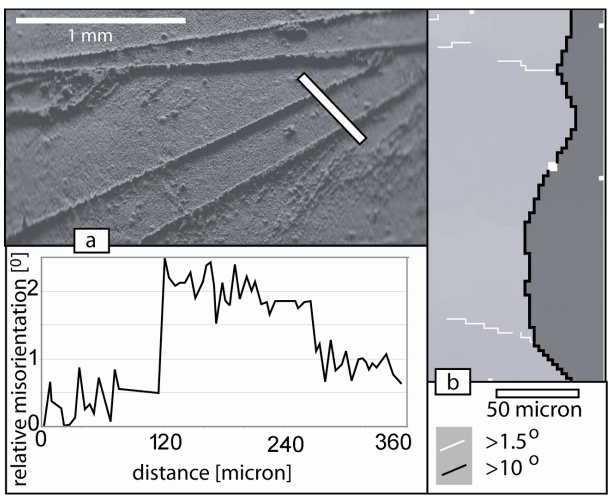

Figure 5 Detailed EBSD analysis from experimentally deformed polycrystalline ice. (a) Subparallel subgrain boundaries as seen in the secondary electron (SE) image. Subgrain boundaries appear as positive features (lines) in such images. Below SE image a transect showing the change in orientation along the white bar shown in SE image from left to right. Note that the two subgrains on the upper left and lower right have a similar orientation. (b) Subgrain boundaries of > 1.5 degrees misorientation developed at an irregular grain boundary. Note that the subgrain boundaries are discontinuous and that their tip is positioned at curvature changes of the grain boundary; different grey scale = different crystallographic orientation.

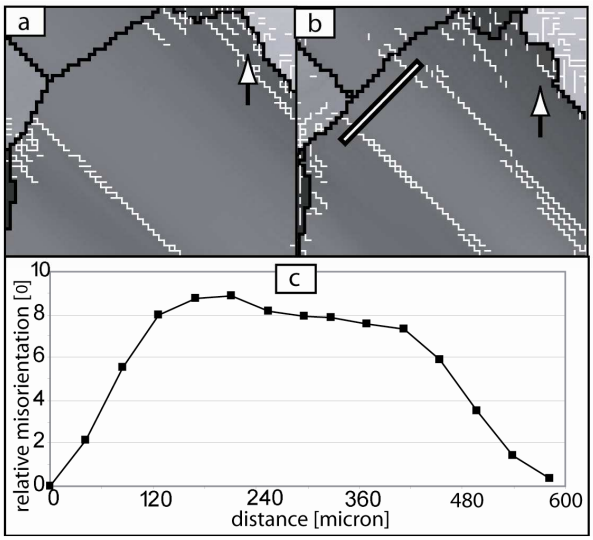

Figure 6 Analysis of two stages of the numerical simulation of polycrystalline ice deformation (2% & 4% strain) showing (I) straight subparallel band development and (II) development of grain boundary asperities at the location of pre-existing subgrain boundaries (arrows). (a) after 2% strain; (b) after 4% strain; different grey scale = different crystallographic orientation. (c) transect showing the change in orientation along the white bar shown in (b) from lower left to upper right.

Summary and Outlook

In this contribution, we can show that the combination of experiments and numerical modelling of experimental observations allows us to develop an in-depth understanding of subgrain scale processes. In the future, scientist can use the models to predict microstructural development and rheological behaviour of a variety of crystalline materials. Nevertheless, it is essential to verify the predicted behaviour through benchmarking physical and numerical experiments.

Acknowledgements:

We thank for financial support the Swedish Research Council (VR 621-2004-5330), the Knut and Alice Wallenberg Foundation (equipment), the ESF through their EUROCORES Programme EuroMinScl, FP6 and the INSIS Institute of CNRS. M. Ahlbom and A. Sundberg are thanked for help in SEM based analyses.

References

[1] R. D. Doherty, D. A. Hughes, F. J. Humphreys, J. J. Jonas, D. J. Jensen, M.E. Kassner, W. E. King, T. R. McNelley, H. J. McQueen, & A. D. Rollett: Mat. Sci. & Eng. A Vol. 238, p. 219 (1997)
[2] B.L. Adams, S.I. Wright, K. Kunze: Metallurgical Transactions Vol. 24A, p. 811 (1993)
[3] D. J. Prior, J.Wheeler, L.,Peruzzo, R., Spiess, C.Storey: J. Struct. Geol. Vol. 24, 999 (2002).
[4] S. Piazolo, M. Montagnat, J.R. Blackford: J. Microscopy Vol. 230, pg. 509 (2008)
[5] S. Piazolo, M. Bestmann, C. Spiers, D. J. Prior : Tectonophysics Vol. 427, p. 55 (2006)
[6] M. Bestmann, S. Piazolo, C. Spiers, D. J. Prior: J. Struct. Geol. Vol. 27, p. 447 (2005)
[7] J.L.Wilson, D.S. Russell-Head, H.M. Sim: Ann. Glaciol. Vol. 37, p.7 (2003)
[8] M.W. Jessell, P.D. Bons, L. Evans, T. Barr, K. Stüwe: Computers & Geosciences Vol. 27, p. 17 (2001)
[9] S. Piazolo, M.W. Jessell, P.D. Bons, L. Evans, J. Becker: J. Geol. Soc. India Vol. 75, p. 110 (2010)
[10] R. A. Lebensohn: Acta Materialia Vol. 49, p. 2723 (2001)
[11] D. Moldovan, D. Wolf, S. R. Phillpot, A. J. Haslam: Acta Mater. Vol. 50, p. 3397 (2002)
[12] D. Moldovan, D. Wolf, S. R. Phillpot: Acta Mater. Vol. 49, p. 3521 (2001)
[13] P. Mansuy, A. Philip, J. Meyssonnier: Ann. Glaciol. Vol. 30, p.121 (2000)

Recrystallization and Grain Growth IV
10.4028/www.scientific.net/MSF.715-716

Substructure Dynamics in Crystalline Materials: New Insight from In Situ Experiments, Detailed EBSD Analysis of Experimental and Natural Samples and Numerical Modelling

10.4028/www.scientific.net/MSF.715-716.502